



A sea bottom classification of the Robredo area in the Northern San Jorge Gulf (Argentina)

N. Sánchez-Carnero¹ · D. Rodríguez-Pérez²

Received: 27 February 2020 / Accepted: 17 December 2020 / Published online: 2 February 2021
© The Author(s), under exclusive licence to Springer-Verlag GmbH, DE part of Springer Nature 2021

Abstract

Benthic habitats are primarily determined by the nature of the substrate (i.e., the type of sediment or rock) and by the bathymetry (e.g., light availability, current, or waves exposition) both determining the viability of infaunal organisms. In this sense multibeam (MB) echosounders provide more data about the sea bottom than any other acoustic technique. During the 2014 Argentine-Canadian survey of the RV Coriolis II in the Gulf of San Jorge, MB data were acquired in the area of Robredo, west of the Marine Protected Area (MPA) *Parque Interjurisdiccional Marino Costero Patagonia Austral* (PIMCPA, Patagonia, Argentina). Acoustic data were affected by acquisition artifacts, so an ad hoc algorithm was required to restore the data. Moreover, during the survey, dredge samples were also acquired where acoustic data suggested changes in substrate properties, and two later scientific surveys acquired video transects of the sea bottom that allowed also a basic classification. A non-supervised classification of the seabed was performed, using a subsampling and voting algorithm, with the acoustic and bathymetric data. The final classification is in agreement with groundtruthing (dredge samples and video transects), showing that bottom structure complexity leads to a meaningful picture of the sea bottom classes in the area. Our results reveal that Robredo has two subareas, one with a fine substrate (west) and another with a coarse substrate (east), the latter being also characterized by outcropping rock formations of marked relief. Despite the small spatial coverage of the survey, the resulting sea bottom classification presented in this paper has described, for the first time, some important features of the benthic geohabitats in the PIMCPA.

Keywords Benthic geohabitat · Multibeam echosounder · Seabed classification · Patagonian Gulf

Introduction

Benthic habitat is primarily determined by the nature of the substrate, sedimentary or rocky structures, configuring the geohabitat, which reflect the physical processes in the near-bottom environment. For example, light availability is associated with bathymetry, wave exposure is associated with the slope and orientation of the sea bottom, the viability of infaunal organisms is linked to sediment granulometry, and nutrient availability is linked to sediment composition. In this sense, the geohabitat determines to a large extent

the presence or absence of a particular benthic species and modifies the effect of disturbances on the benthic community (Greene et al. 1995; Auster and Langton 1999; Guisan and Zimmermann 2000). The characterization of the seabed in terms of terrain parameters such as slope, aspect, or curvature may therefore offer us a valuable tool for delineating areas of the continental shelf that are likely to support particular fauna and thereby provide a distinct geohabitat (Wilson et al. 2007; Brown et al. 2011; Lucatelli et al. 2019), thus improving our understanding of ecosystem dynamics (Pickrill and Todd 2003; Pandian et al. 2009; Brown et al. 2011; Bosman et al. 2020).

In the last decades, multibeam echosounders (MBES) have gained broad acceptance as a means to acquire high quality seafloor data, and are today recognized as the most effective tools to map the seafloor, being used in different applications, such as geomorphological and geomorphometric characterization (Normandeau et al. 2014; Normandeau et al. 2015; Lecours et al. 2016; Picard et al. 2018), geohabitat mapping (Van De Beuque

✉ N. Sánchez-Carnero
noelas@gmail.com

¹ Centro para el Estudio de Sistemas Marinos (CESIMAR), CCT CONICET - CENPAT, Puerto Madryn, Argentina

² Departamento de Física Matemática y de Fluidos, Facultad de Ciencias, Universidad Nacional de Educación a Distancia (UNED), Madrid, Spain

et al. 1999; Kostylev et al. 2001; Parnum et al. 2004), benthic fauna distribution (Kostylev et al. 2003; Roberts et al. 2005; Mcgonigle et al. 2009), archaeological remains identification (Singh et al. 2006), and scientific investigation of the Earth's crustal deformations (Calder and Mayer 2003). MBES have rapidly evolved into sophisticated instruments capable of synthesizing hundreds of very narrow beams, allowing them to cover a wide swath (full coverage) (Le Bas and Huvenne 2009) with a very high spatial (vertical and horizontal) resolution. MBES systems allow co-registration of bathymetry and backscattering data with similar resolutions (Clarke et al. 1996; Pickrill and Todd 2003); thus, the ability to acquire both informations together makes MBES the reference tool for sea bottom mapping (Brissette and Clarke 1999; Brown et al. 2011).

Often, interpretation of sea bottom data is conducted visually using acoustic backscatter and bathymetry data (Bosman et al. 2020; Kanari et al. 2020), underwater video (Edwards et al. 2003), or a combination (Fontelles Ternes et al. 2019). However, manual segmentation is inherently subjective, slow, and potentially inaccurate (Cutter et al. 2003) which is problematic in view of the subtle variations that may be present in acoustic responses and the large volumes of data being collected during surveys (Brown and Collier 2008; Blondel and Gómez Sichi 2009). As a consequence, some authors addressed the need of developing quantitative, robust, and efficient techniques to analyze MBES data (Cutter et al. 2003; Fonseca et al. 2009; Micallef et al. 2012; Stephens and Diesing 2014). Currently, it is an advancing field in which several approaches are being tested: supervised and unsupervised classification using bathymetric variables including or not backscattering strength (Micallef et al. 2012; Rattray et al. 2013; Li et al. 2017; Pillay et al. 2020), backscattering angular response (Simons and Snellen 2009; Che Hasan et al. 2014), multiscale analysis (Misiuk et al. 2018), and textural analysis (Blondel and Gómez Sichi 2009).

Although there are many countries which use MBES routinely like the USA (Whitmire et al. 2007), Canada (Brown et al. 2011), the UK (Kostylev et al. 2001; Brown et al. 2002; Mcgonigle et al. 2009), France (Lurton et al. 2018; Fezzani and Berger 2018), or Australia (Rattray et al. 2009; Che Hasan et al. 2012), there are many others where MBES have never been used but for some scarce opportunities. This is the case of Argentina where, in spite of its ecologically relevant continental platform, its fishing resources, and the economic importance of oil extraction, the MBES soundings found in the scientific bibliography are limited to a few technical reports (Madirolas et al. 2005) and scientific papers (Lastras et al. 2011; López-Martínez et al. 2011; Borisov et al. 2014).

Thus, a new opportunity arised in 2014 in the framework of the Argentine-Canadian MARGES expedition when a

MBES acoustic survey was conducted in some areas of the San Jorge Gulf by the research vessel Coriolis II. The opportunity consisted in surveying for the first time a marine area whose biodiversity and economic activity are very important (it is one of the most important South-West Atlantic fisheries), but whose sea bottoms are almost unknown. The continental part of the San Jorge Gulf shows a series of diverse geological structures (rhyolitic lavas and pyroclastic flow deposits; Lema et al. 2001) belonging to the Marifil Formation, part of the Large Igneous Province (LIP) Chon Aike, that runs from Patagonia to Antarctica (Pankhurst et al. 1998). Moreover, the submerged area is expected to combine this geomorphological richness (Haller et al. 2020) with a considerable presence of sediments deposited along the ages by transport processes conveying continental material and by the biodegradation of the Gulf fauna (Desiage et al. 2018).

After expedition, on-shore analysis of the MARGES data showed that the MBES data was corrupted due to a misconfiguration of the inertial motion unit (IMU) and a mismatch between the sound velocity profile and the sound surface velocity input to the echosounder in order to conform the acoustic beams. These errors introduced undulations in the bathymetry and in the backscattering strength that could not be corrected with usual softwares, so an ad hoc correction would be required to approach the level of detail potentially obtained with an MB. This is especially important in this area, because it spans a small area which mapped in large pixels (that would average out those undulations) would not reveal the detail structures that characterize its bottom geomorphology. Moreover, this characterization is important in an area where bottom information is scarce, and when the possibility of obtaining new MB data is remote.

Given that the MARGES was the very first MB study of the bottoms in this ecologically important area, developing a sea bottom classification is still an attractive goal for the sea floor habitat community even if the results are not as good as initially planned for the MB survey, because it will be far more detailed than any previous study in the area. Mapping the (small) surveyed area in large pixels (that would average out the undulations) is not an option, as that would not reveal the detail structures that characterize bottom geomorphology. Hence, with the aim of “making weak data good”, an ad hoc correction was performed, prior to classification to approach the level of detail potentially expected from the MB.

The goal of this paper is to generate from the available MB data the first bathymetric and acoustic map of the area of Robredo, in the Marine Protected Area (MPA) established in the north of San Jorge Gulf (Patagonia Argentina), based on unsupervised analysis of backscattering strength, and bathymetry derivative variables.

Methodology

Study area

The study area is located in the northern coastal zone of the San Jorge Gulf, a semi-open basin with an extension of 39,340 km², between 45° S (Cape Dos Bahías) and 47° S (Cape Tres Puntas) (Fig. 1). The Gulf seafloor is dominated by coarser sediments on the northern coast, whereas finer sediments prevail in the north-central area, and even finer fractions towards the inner part of the Gulf (Fernández et al. 2003; Desiague et al. 2018). It is a fishing ground, a breeding and spawning area of several fish and crustacean species including the commercial shrimp *Pleoticus muelleri* and the hake *Merluccius hubbsi* (Bertuche et al. 2000). The San Jorge Gulf is highly exposed to environmental risks related to the urban-industrial oil production hub of Comodoro Rivadavia, with prospective offshore drilling, and intense shipping activity (Nievas and Esteves 2007). This oil production coexists with major commercial fisheries (Gongora et al. 2012) and with areas of great significance for marine conservation because of the presence of reproductive aggregations and foraging grounds of many marine birds and mammals (Blanco and Quintana 2014; Grandi et al. 2015).

In the northern area of the Gulf, the MPA *Parque Interjurisdiccional Marino Costero Patagonia Austral* (PIMCPA) was established in 2007 and trawl fishing was prohibited in 2013 (Fig. 1). The MPA is one of the most relevant areas of the Argentine coast in terms of biodiversity and productivity and a management plan is being developed for it, involving government representatives and scientists. Although there are several studies about distribution of seabirds and marine mammals in this area and the effects of human activities on the depletion or recovery of their populations (e.g., Yorio 2000, 2009; Copello and Quintana 2009; Blanco and Quintana 2014; Grandi et al. 2015; Romero et al. 2017), the knowledge about sea bottom characteristics is scarce, not to mention the knowledge about the distribution of benthic communities and the impact that fishing gears have on them.

The focus of our work will be in the area of Robredo located northwest of the San Jorge Gulf, an area that has been under fishing pressure nearby the southern boundary of the PIMCPA (Fig. 1).

Data acquisition

The acoustic survey was conducted during the campaign of the research vessel Coriolis II on February 23th and 24th

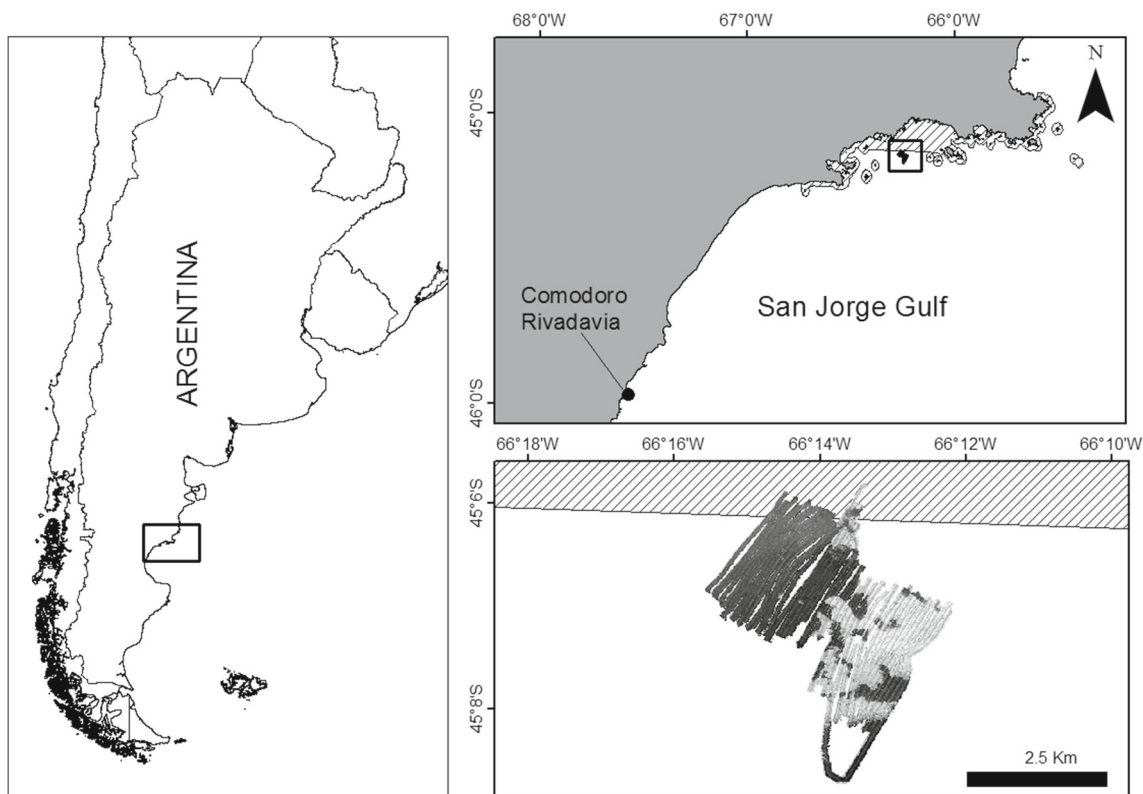


Fig. 1 Study area in the North of the San Jorge Gulf (Patagonia, Argentina). The marine national park (*Parque Interjurisdiccional Marino Costero Patagonia Austral*) is shown (striped area) and the acoustic transects in the Robredo area are shown South of this area

2014 as part of the MARGES expedition (St-Onge and Ferreyra 2018).

Fifty acoustic transects were performed using a Kongsberg EM2040 multibeam echosounder, covering a depth range between 25 and 70 m obtaining a 100% coverage. The sounder operated with frequencies of 300 kHz, producing 256 beams of 0.5° in the alongship direction, and with “equispaced tangents” in the athwartship direction, with a total swath width of 140° (that is, being the swath of seafloor image 5.5 times the water depth). The pulse length was 70 μ s (CW mode) potentially achieving a vertical resolution of approximately 5 cm at nadir and 18 cm at the outer beams (in the deepest area), and a horizontal resolution (in the deepest area) around 1.5 m (along the entire swath, also in the deepest area). The vessel ran the survey at 5 kn and the position data were provided by a POS MV 320 differential Global Positioning System (dGPS), providing a positional accuracy of 0.5–2.0 m. A total of 4 sound velocity profiles (SVP) were collected during the survey (one about every four hours) using an SBE 911plus CTD.

Granulometry

Along with the acoustic data, bottom samples were taken at 12 sites. The sites were chosen by on line visual interpretation of the MBES backscatter image at places where changes were visible in the sea bottom (circles in Fig. 4). Samples were obtained with a van Veen dredge of 0.008 m^3 and were used afterward to characterize bottom granulometry. For each sampled point, sediment samples corresponding to the sediment/water interface were collected. All samples were carefully labeled and the whole process was photographed.

Sediment samples were dried in an oven at 80°C for around two days until they reached a stable weight. Particle size range and size distribution of the different samples was determined through analytical sieving, using a vibration screen Zonytest sieve (4000 μm , 2000 μm , 1000 μm , 500 μm , 250 μm , 105 μm and smaller), and then classified according to the Folk classification as mud, fine sand, coarse sand or rock.

Video transects

In two surveys conducted in March and May 2016, 6 bottom video transects and other two local video recordings were acquired using a drift imaging system (Trobiani and Irigoyen 2016). The imaging system had two cameras, one aimed at the bottom, used for data acquisition, and another one pointing horizontally forward (called explorer camera), used to control the height of the imaging system above the ground to avoid potential collisions. The imaging system was trawled by a vessel over the bottom using a pair of steel

wires, one of them holding a Foiled Twisted Pair (FTP class 5) for data transmission to the surface.

From the geolocated video footages acquired by the bottom camera, a visual sea bottom classification was performed classifying 100 m subtransects as muddy, sandy or rocky, according to the most relevant class (Trobiani 2018); each of these subtransects was mapped to its central point (squares in Fig. 4).

Acoustic data processing

Multibeam data are acquired at potentially very high spatial resolution. In a common survey, a series of corrections are needed to reduce artifacts due to variations in sound velocity profile, tidal height (using data from a nearby reference harbor), vessel attitude oscillations (measured by the IMU), etc. that could hinder features that characterize the sea bottom. These corrections are usually followed by visual inspection and manual edition to detect and remove other errors (e.g., false bottom detection). In this work, all this processing of the acoustic data was performed using CARIS HIPS & SIPS version 9.0, using as input the MBES, IMU and SVP data acquired during the survey, and the tidal height, adjusted by spline interpolation, from that of the main harbor in the San Jorge Gulf, Comodoro Rivadavia. However, in our case, an IMU misconfiguration during the survey and the error in surface sound velocity, made these corrections inaccurate.

Hence, after conducting the usual corrections an ad hoc correction was performed in order to reduce the most visible remaining artifacts (small or medium undulations throughout the swath in a counter-phased pattern and mismatch between contiguous transects). This ad hoc correction (see Fig. 2) consisted in a curvature filter that minimized the undulations in the depth data, and a similar curvature correction plus a beam pattern subtraction, applied to correct the artifacts in the backscattering data. The ad hoc correction was implemented using the R statistical package (R Core Team 2019) and Octave (Eaton et al. 2019).

To correct the undulation artifact, we mapped the XYZ coordinate record of each transect onto a raster map M . Given that the undulations manifested as quasi-periodic changes in the surface curvature, we computed the maximum curvature of the surface locally rendering a maximum curvature map C that highlighted the artifacts. Then, we added $M' = M + \alpha C$ with an α such that the resulting mean square curvature was minimum for each transect. The result was a mosaic of curvature corrected transects mapped on a 5×5 -m grid with minimal overlap errors.

The sea bottom backscatter strength (BS) computed by CARIS showed two types of errors: modulations of BS

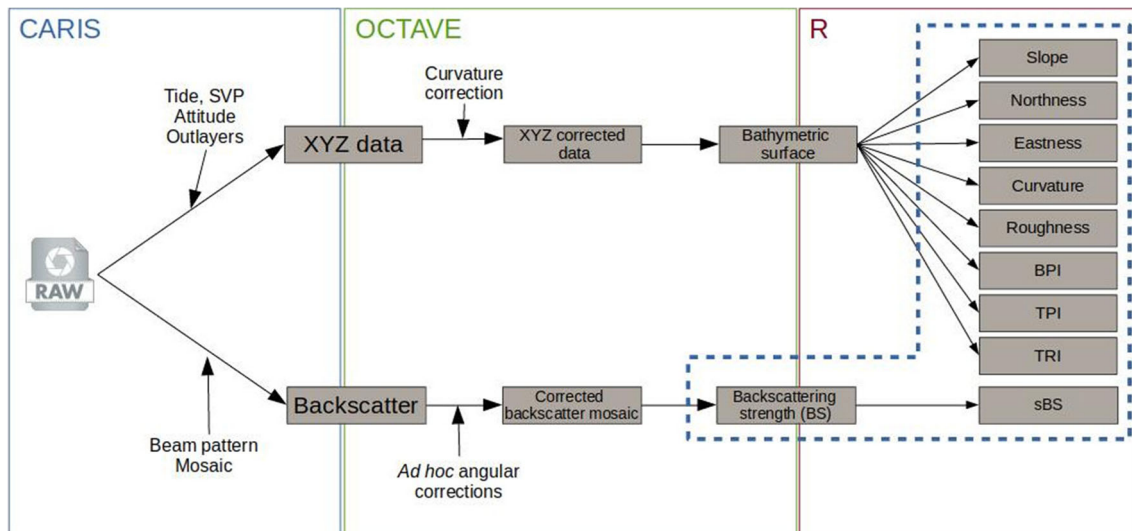


Fig. 2 Workflow from acoustic raw files to bottom-derived variables

following the bathymetric undulations, and strong variations of BS along the swath of the transects. To correct the latter effects, a beam pattern correction was performed (Le Bas and Huvenne 2009; Che Hasan et al. 2014). For each beam b in the MB swath, the average BS value \overline{BS}_b was computed over the entire transect, then the average over all beams \overline{BS} was computed. The correction consisted in subtracting the value $dBS_b = (\overline{BS}_b - \overline{BS})$ to the corresponding beam signal recorded in each transect. After these corrections, a BS mosaic 5 m in resolution was obtained projecting all transects over a 5×5 -m raster grid.

Seabed classification

Unsupervised seabed classification was performed using as input variables the backscattering strength (BS) and its local standard deviation (sBS) together with the 8 bathymetry-derived variables summarized in Table 1, computed in order to characterize the shape and variability of the sea bottom. Raster maps of these bathymetry-derived variables (5 m pixel size) were computed based on definitions taken from the bibliography (Wilson et al. 2007; Ierodiaconou et al. 2011; Micallef et al. 2012; Stephens and Diesing 2014; Calvert et al. 2015; Lecours et al. 2016).

A subsampling and voting classification algorithm using k-means (Hartigan and Wong 1979) was used, successively applying the following steps 10 times:

1. a random sample of 10% of the pixels was selected (with replacement);
2. the values of the variables in that sample were de-correlated using a principal component analysis (PCA);

3. a k-means algorithm was applied to these components, giving the centroids of the classification;
4. every pixel in the whole raster was assigned to the class of its nearest centroid thus generating a classification map.

Of all these 10 classification maps, the class most frequently assigned to each pixel was taken as its most probable classification, rendering the final classification map. The interpretation of this unsupervised classification was done based on the statistics of the most relevant variables in each class, as well as from the comparison with groundtruthing samples and video transects included within each class.

Results

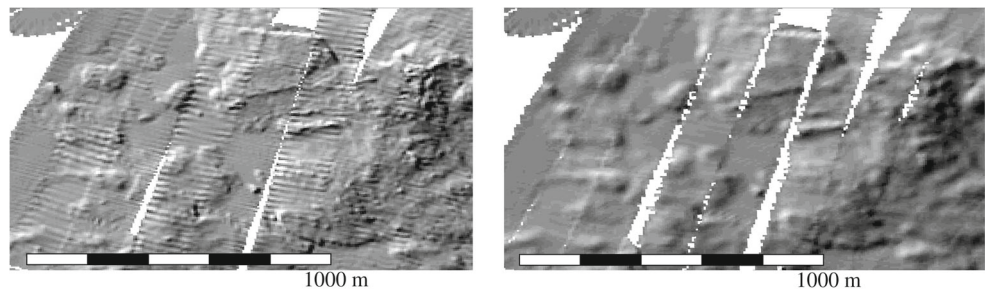
The first results presented are the bathymetry and backscattering data which illustrate some geomorphological properties of the seabed. The ad hoc correction removed successfully most undulation artifacts at the cost of slightly smoothing out actual features. Figure 3 shows an example of uncorrected and corrected bathymetries in the eastern part of the study area; for the backscattering strength the results are similar.

Bathymetric data (Fig. 4—left) show the seabed ranged from 68 m (in the South) to 27 m (in the North), although there is also a (rocky) formation in the Central East part that emerges to 22 m. Backscatter data (Fig. 4—right) revealed two acoustically hard bottom patches over the eastern half of the surveyed area of Robredo ($BS > -20$ dB). These acoustically hard bottoms can be interpreted as a basement high composed of Jurassic rocks of the Marifil

Table 1 Multibeam sonar variables and derived geomorphometric features used for classification

Variable	Code	Description	Horizontal range
Slope	SL	Maximum rate of change in elevation around a cell, related with the departure from horizontal.	5 × 5 cells
Northness	NO	Cosine of the orientation of the slope measured from East, related with exposure to prevailing swells or currents.	5 × 5 cells
Eastness	EA	Sine of the orientation of the slope measured from East, related with exposure to prevailing swells or currents (linearly independent from Northness).	5 × 5 cells
Curvature	CUR	Sum of the second derivatives of the bathymetry (mean curvature), related with surface deformation (concavity or convexity).	5 × 5 cells
Roughness	RO	Difference between the maximum and minimum depth values in a specific neighborhood around a cell, related with structural complexity.	5 × 5 cells
Bathymetry Position Index	BPI	Absolute value of the difference between cell depth and the mean depth of its neighborhood (i.e., absolute value of TPI), related with local surface variability.	5 × 5 cells
Topographic Position Index	TPI	Difference between cell depth of each cell and the mean depth of a specific neighborhood around, related with local surface variability.	5 × 5 cells
Topographic Roughness Index	TRI	Mean square difference between a point's height and the heights in its neighborhood, related with structural complexity.	5 × 5 cells
Backscatter	BS	Average backscatter strength (in dB) in a cell, related with the acoustic impedance/hardness of the bottom.	1 cell
Backscatter typical deviation	sBS	Standard deviation of the backscatter strength in a neighborhood around a cell, related with the acoustic nonhomogeneity/roughness.	7 × 7 window

Fig. 3 Multibeam bathymetry in a region of Robredo, before (left) and after (right) the maximum curvature ad hoc correction. Bathymetry shadows have been equally exaggerated in both images to highlight all the artifacts



Formation described by Lema et al. (2001) outcropping above the generally muddy and sandy bottom. In the absence of riverine flows, coarse and medium sandy bottoms can be interpreted as originated from beach and cliff erosion, while finer portions have been suggested to originate as wind-blown dust from nearby dune fields (Desiage et al. 2018).

Derived variables highlight the differences in bottom structure: only 30% of the area has slopes of 1% or less (mostly in the Northwest) and these slopes are oriented preferentially eastward. Accordingly, terrain roughness, indicating the richness of bottom structure, is also low

(0.023 median): 80% of pixels have roughness under 0.82 m, rougher parts are observed to the East. This distribution of bottom roughness grossly coincides with the areas having higher backscattering levels.

The principal component analysis of the acoustic+bathymetric variables showed that the 3 first components explained 73% of the variance, so only 3 components were used in the classification. Regarding the weight of the variables in these components, TPI, SL and RO were the ones contributing more weight (followed by TRI, BS, BPI and mean curvature); the BS standard deviation weighted low in all three components.

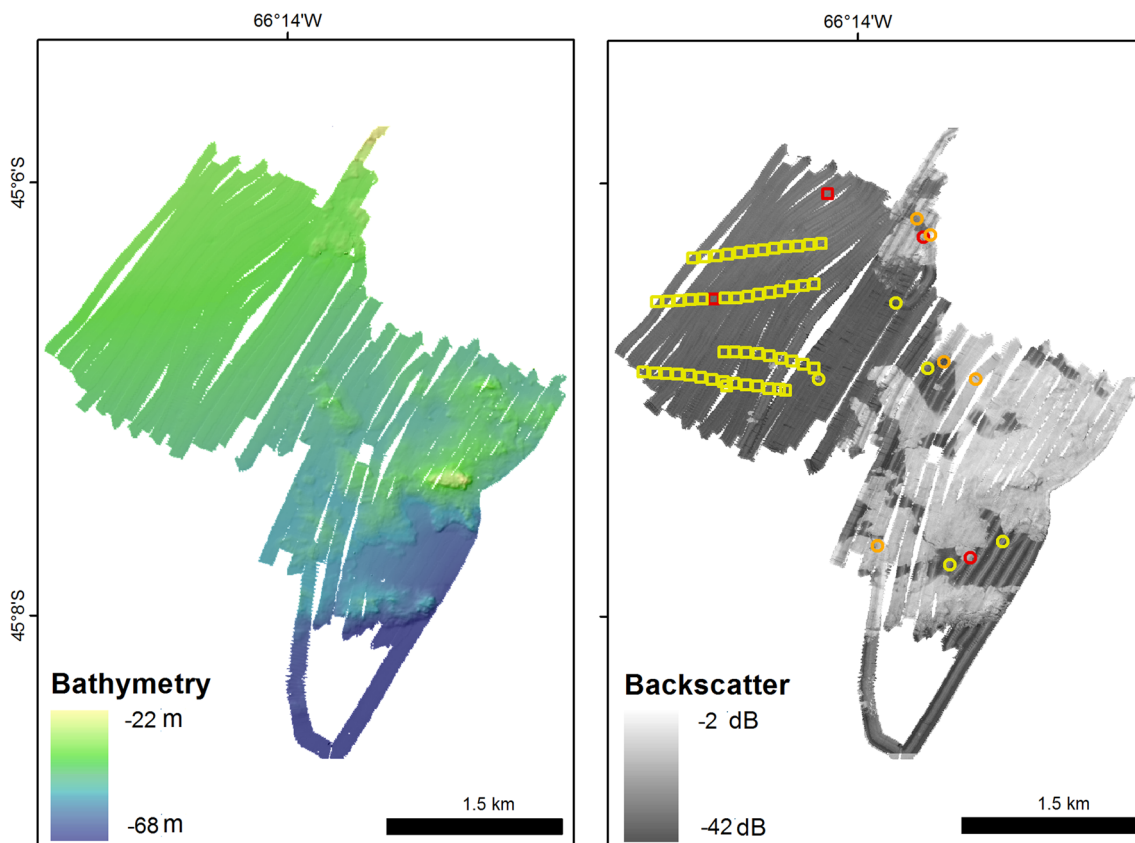


Fig. 4 Results of the acoustic survey: bathymetry (left) and backscatter (right). Groundtruthing sampling locations are displayed as disks and video transect centroids are displayed as squares: yellow

corresponds to fine sediments, orange to medium or coarse sand, and red to gravel or rocky bottoms

Classification

Although sample classifications used five classes, the final voting step removed one of them because of its instability; hence, only 4 classes remained, as shown in Fig. 5. The classes were numbered in terms of their extension from 1 (the most abundant) to 4 (the less abundant) as RB-1, RB-2,... The unsupervised classification reflects the differences in the values of acoustic and bathymetry derivative variables in the area (see Table 2).

In the classification, bathymetry derivatives become the most important features that determine classification. In the western area, class RB-1 is dominant (see Fig. 5). Class RB-2 appears in the boundaries of RB-1 transects in the western

area, and should be interpreted there as the same class RB-1 (pointing out to an artifact related with corrections in that part of the area). In the eastern part, classes RB-2, RB-3 and RB-4 are the most frequent, although two RB-1 patches appear in the southern half. The class RB-4 appears marking ridges within the RB-3 patches, and could be interpreted as the same class RB-3, particularized within some particular geomorphologic features (see Table 2).

Groundtruthing and bottom class interpretation

Granulometric classification of samples in areas of class RB-1 corresponds mostly to silt or fine sand according to Folk's classification. The samples within areas of class

Fig. 5 Seabed classification. Classes have been labeled in terms of their extension (1, largest, to 4, smaller) and are denoted by different colors

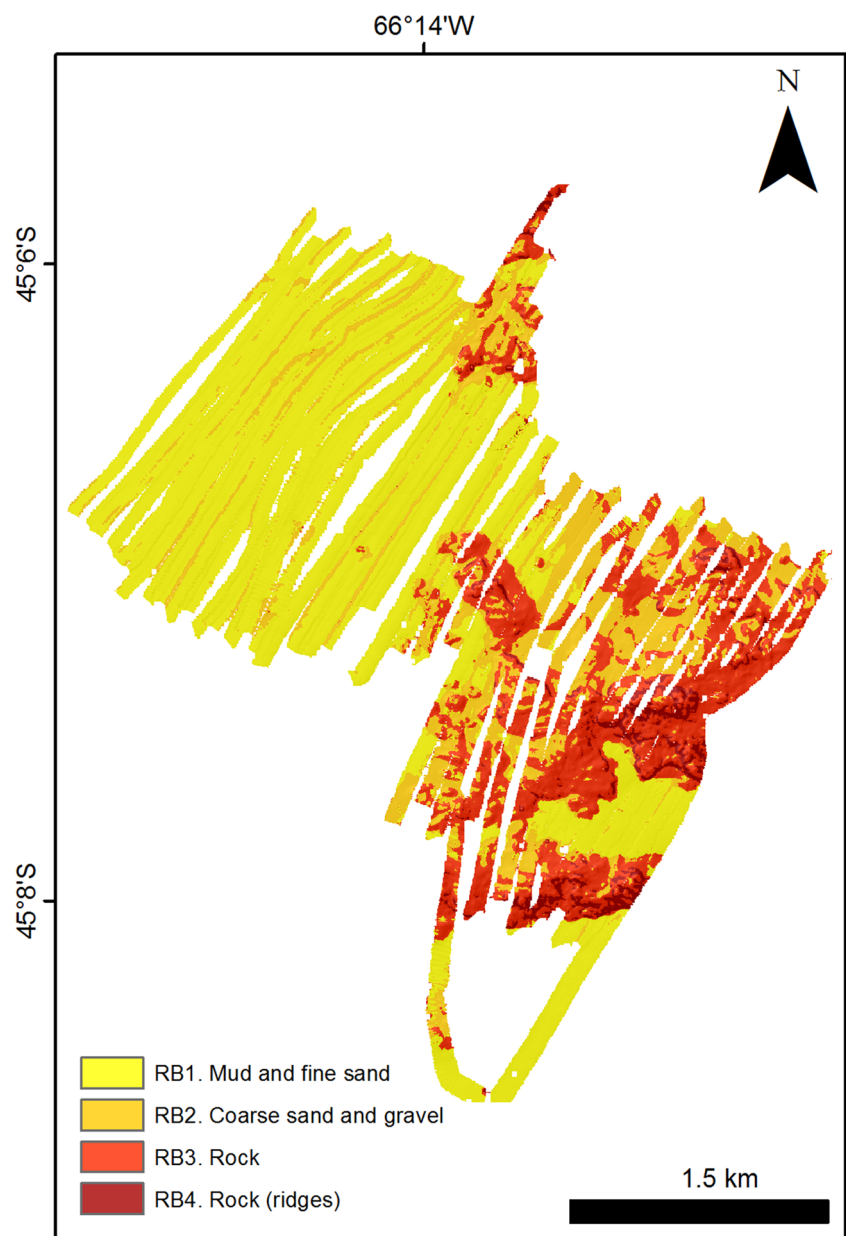


Table 2 Values of representative variables per class (Q1, Q3: first and last quartiles) together with their interpretation in terms of groundtruthing sample classification (illustrated by photographs: superposed rulers are 10 cm in all images)

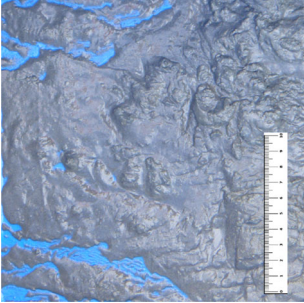


Bottom type	Class	slope (%)			RO (m)			TRI (m)			BS (dB)		
		Q1	Median	Q3	Q1	Median	Q3	Q1	Median	Q3	Q1	Median	Q3
Mud and fine sand	RB-1	0.29	0.43	0.65	0.098	0.136	0.196	- 0.011	- 0.000	0.010	- 25.6	- 24.5	- 23.2
													
Coarse sand and gravel	RB-2	0.36	0.68	1.20	0.144	0.224	0.351	- 0.016	0.002	0.023	- 23.2	- 17.8	- 13.3
													
Rocky bottom	RB-3	1.60	2.42	3.44	0.449	0.654	0.907	- 0.043	- 0.004	0.030	- 14.8	- 13.5	- 12.4
													
Rocky bottom (ridges)	RB-4	5.08	6.35	8.33	1.313	1.631	2.137	0.036	0.087	0.140	- 16.5	- 14.2	- 12.9

Table 3 Contingency table of the classification

	RB-1	RB-2	RB-3,4
Mud-fine sand	54	1	0
Coarse sand-Gravel	0	5	0
Rock	2	1	1

Rows: groundtruthing classes (bottom samples and underwater videos). Columns: classes from the unsupervised classification (accuracy: 0.94; kappa: 0.74)

RB-1 correspond to mud and fine sand, although some of them lay close to boundaries between RB-1 and RB-2 classes. The samples of coarse and very coarse sand or fine gravel lay close to class RB-3 and RB-4 patches. The only samples classified as rock (two from bottom samples and two from video transects) are either included in the same class as hard substrates or in a complex region with nearby pixels classified in three or more different classes.

The video transects mostly cover the area classified as class RB-1, being most of the transects visually classified as mud, but for two where rocks were observed (Fig. 4—right squares). Table 2 summarizes both the granulometric and video correspondences with the unsupervised classification. After labeling the classes according to the most abundant sample class (mud/fine sand, coarse sand, or rock), the classification accuracy was found as 0.94, with a kappa of 0.74 (see contingency Table 3).

Discussion

In the previous sections, we have presented a classification of the benthic geohabitats in the area of Robredo, part of the Marine Protected Area *Parque Interjurisdiccional Marino Costero Patagonia Austral* (PIMCPA), based on the data acquired during the Argentine-Canadian Coriolis II survey of 2014. The final classification (see Fig. 5) reflects not only the granulometry but also the bottom structure complexity, and shows how both features are related (see Table 2).

Ad hoc data correction

MB data correction has been extensively treated (see Clarke 2003 for a systematic analysis) and robust algorithms have been developed and implemented in softwares like CARIS to obtain geometrically and acoustically corrected data. However, when a data set has acquisition errors, as in this study, these standard corrections are not enough, and wavy patterns remain. Other authors have dealt with similar problems and all of them have proposed their own solutions

(Yang et al. 2007; Beaudoin et al. 2018). In our case, however, the corrections were more demanding because acquisition errors were larger and our study area had regions of very homogeneous sea bottom, with very small relief, making the systematic errors even more visible in the data (see Fig. 3 left). Backscattering artifacts were smaller and usual corrections worked better. In this case, homogeneous and flat seabed provided a full range of backscatter returns collected at different angles and ranges valid to perform a pseudo-calibration that compensated transducer directivity and seafloor incidence (angular dependencies; Le Bas and Huvenne 2009; Chakraborty et al. 2003). However, despite this equalization, slightly higher BS levels still remained at the center of the transects, something commonly observed in previous studies. However, this small difference was not large enough to introduce artificial “center of transect” classes in soft bottom areas (as an acoustic-only classification would have).

Classification

Many recent studies have applied multivariate statistical methodologies to solve the problem of automatic classification of the seabed using MBES data (Brown and Blondel 2009; Shumchenia and King 2010; Heap and Harris 2011; Che Hasan et al. 2012; Che Hasan et al. 2014; Li et al. 2017; Pillay et al. 2020 and references therein). Despite all statistical methodologies (often labeled as machine learning), no technique has singled out as the gold standard in geohabitat classification although some of them have given good results such as classical k-means or random-forests (see Pillay et al. 2020 for a recent comparison). We have opted for an off the shelf approximation based on lessons learned from the bibliography: a principal component analysis to de-correlate variables (necessary when using bathymetry derivatives), a k-means clustering with a reasonable number of classes (a larger number increased the patchiness of the results, breaking the spatial coherence; a smaller number, just selected two stable classes), and then a voting algorithm to assure the robustness of the resulting classification. Some authors (Fonseca et al. 2009; Micallef et al. 2012; Fontelles Ternes et al. 2019) have noticed that BS is a very good predictor of the sea bottom type, related with granulometry, whereas other authors have shown that including bathymetric variables actually improves the seabed classification (Roberts et al. 2005; Pirtle et al. 2015). In our case, BS ranks low in the list of informative variables, and is not among the topmost 3 (that are slope, TRI and roughness). This difference could have its origin in the remaining uncorrected errors of BS, but also in the geomorphology of our study area, where the existence of flat sedimentary areas and high slope rocky areas, makes variables as slope or roughness very informative. This is particularly visible in

acoustically harder (coarser) substrates where a geomorphological feature as TRI improves the boundaries definition and classification accuracy (Rattray et al. 2009; Calvert et al. 2015).

Regarding the level of agreement achieved with the classification, accuracy was 0.94 which is comparable to values obtained in previous works using MB to classify sea bottom (Che Hasan et al. 2012; Diesing and Stephens 2015). These works usually employ supervised classifications with large number of groundtruthing points, and vary in their number of classes (from 2 to 4, not counting mixture classes) and accuracies. To take into account statistical sampling bias, Cohen's kappa was computed as 0.74, that assures a substantial correspondence between classification and field data (that value is in the interval of kappa values reported in the preceding works). The difference between accuracy and kappa is due to the differences in extension of the different bottom classes, and also the unbalanced number of groundtruthing points over each bottom type. Specifically, in our case, rocky and coarse sediment bottoms are underrepresented in videos and granulometry points: only 4 rocky and 5 coarse sediment samples, against 55 of muddy and fine sand. Conversely, both fine and coarse sediment points showed a very good agreement with the classification, while rocky samples fall off the areas classified as rock. One reason for this latter mismatch is that sampling at the exact location of a rocky outcrop over a sandy bottom is difficult; that was the case in 2 video transects classified as rock, because they showed isolated rocks over a sandy/muddy bottom (in the western part of Robredo). Another reason are heterogeneous areas, where in a few meters alternate rock and gravel; this was the case in other 2 sampling points in the eastern part of Robredo.

Despite the evident improvement in the input data after the ad hoc correction (see Fig. 3 right), the final effect on the classification is difficult to assess. First, because the overall classification applied to the raw uncorrected data showed a spatial distribution similar to Fig. 5, and second, because validation using our groundtruthing data does not show more significant mismatches in one case or in the other.

Bottom cartography

Interpretation of the obtained acoustic classification has led us to a spatially consistent map of the sea bottom, labeling the classes according to their geomorphologic characteristics as fine sediments, coarse sediments, rocky bottoms and rocky ridges (Fig. 5). In this map of Robredo we can identify two well-differentiated areas: one with a predominantly fine substrate to the west, and one with a coarser substrate to the east, presenting the latter two rocky formations with marked relief. These geomorphological

structures are related with the continental relief, whose continuation underwater was unknown until now.

Although most geohabitats are related to granulometry, other features may determine different geohabitats and, in many cases, substrate and habitat bear a many-to-one relationship (Mcgonigle et al. 2009). Thus, we cannot directly interpret the obtained classification as benthic habitats although some inferences can be done: for example, in other Patagonian coastal areas with similar rocky reefs, there exist fish assemblages characterized by a low diversity and the dwelling dependence of the most abundant species, which are not found beyond a few meters from reef holes and crevices (Galván et al. 2009; Irigoyen et al. 2011). This information represents, thus, a key piece of information for management of the PIMCPA.

Conclusions

In this paper we have generated the first bathymetric and acoustic map of the area of Robredo, near the PIMCPA in the north of the San Jorge Gulf, using multibeam data. Although the MB potential spatial resolution is very high, problems during the acquisition made necessary some ad hoc corrections and caused the loss of horizontal resolution.

The unsupervised classification computed from the bathymetric and backscattering surfaces led to a 4 class bottom cartography covering an area of 10 km² which, according to the groundtruthing data available, rendered an accuracy of 0.94 ($\kappa = 0.74$). The cartography revealed two main well-differentiated areas: one in the nor-western part of the study area, with smooth relief and formed by very fine substrates, where no structures emerged over the bottom, and another one in the south-western part, having coarse substrates and presenting two rocky formations with marked relief and slopes up to 8%, that are the continuation of the chain of small rocky islands that exist in the PIMCPA.

This information represents the most detailed cartography to date in all the area, and is a key piece of information for managing a marine area as ecologically and economically relevant as the PIMCPA.

Acknowledgments The authors wish to thank the captain, officers and crew of the RV Coriolis II for their support during the field campaign, Pierre-Arnaud Desiège for his help in the data acquisition, Mathieu Rondeau (at CIDCO) for his help with CARIS and multibeam data correction, Dr. Alejo Irigoyen and Dr. Gaston Trobbiani for providing the underwater video, and helping with the grain size analyses, and especially, to G. St-Onge, who collaborated both financially and critically in the development of this work and in the preparation of the manuscript. The authors also acknowledge the financial support for the MARES and MARGES expeditions that was provided by the *Ministerio de Ciencia, Tecnología e Innovación Productiva* (MINCyT), *Provincia de Chubut* and *Consejo Nacional de*

Investigaciones Científicas y Técnicas (CONICET) in the framework of the Pampa Azul initiative.

Compliance with ethical standards

Conflict of interest The authors declare that they have no conflict of interest.

References

- Auster PJ, Langton RW (1999) The effect of fishing on fish habitat. In: Fish habitat: essential fish habitat (EFH) and rehabilitation
- Beaudoin J, Renoud W, Haji Mohammadloo T, Snellen M (2018) Automated correction of refraction residuals. In: HYDRO18 conference
- Bertuche D, Fischbach C, Roux A, Fernandez M, Piñero R (2000) Langostino Pleoticus muelleri, Publicaciones Especiales INIDEP. Mar del Plata, pp 179–190
- Blanco GS, Quintana F (2014) Differential use of the Argentine shelf by wintering adults and juveniles southern giant petrels, *Macronectes giganteus*, from Patagonia. *Estuarine, Coastal and Shelf Science* 149:151–159. <https://doi.org/10.1016/j.ecss.2014.08.014>
- Blondel P, Gómez Sichi O (2009) Textural analyses of multibeam sonar imagery from Stanton Banks, Northern Ireland continental shelf. *Applied Acoustics* 70(10):1288–1297. <https://doi.org/10.1016/j.apacoust.2008.07.015>. <http://linkinghub.elsevier.com/retrieve/pii/S0003682X0800203X>
- Borisov D, Murdmaa I, Ivanova E, Levchenko O (2014) Giant mudwaves in the Northern Argentine Basin : born and buried by bottom currents. *Geophysical Research Abstracts* 16(14):31357
- Bosman A, Romagnoli C, Madricardo F, Correggiari A, Remia A, Zubalich R, Fogarin S, Kruss A, Trincardi F (2020) Short-term evolution of Po della Pila delta lobe from time lapse high-resolution multibeam bathymetry (2013–2016). *Estuar Coast Shelf Sci* 233:106533. <https://doi.org/10.1016/j.ecss.2019.106533>
- Brissette M, Clarke JE (1999) Side scan versus multibeam echo sounder object detection: comparative analysis. *Int Hydrogr Rev* 76(2):21–34
- Brown C, Cooper K, Meadows W, Limpenny D, Rees H (2002) Small-scale mapping of sea-bed assemblages in the eastern english channel using sidescan sonar and remote sampling techniques. *Estuar Coast Shelf Sci* 54(2):263–278. [10.1006/ecss.2001.0841](https://doi.org/10.1006/ecss.2001.0841)
- Brown CJ, Blondel P (2009) Developments in the application of multibeam sonar backscatter for seafloor habitat mapping. *Applied Acoustics* 70(10):1242–1247. <https://doi.org/10.1016/j.apacoust.2008.08.004>. <http://linkinghub.elsevier.com/retrieve/pii/S0003682X0800176X>
- Brown CJ, Collier JS (2008) Mapping benthic habitat in regions of gradational substrata: an automated approach utilising geophysical, geological, and biological relationships. *Estuarine, Coastal and Shelf Science* 78(1):203–214. <https://doi.org/10.1016/j.ecss.2007.11.026>. <http://www.sciencedirect.com/science/article/pii/S0272771407005288>
- Brown CJ, Smith SJ, Lawton P, Anderson JT (2011) Benthic habitat mapping: a review of progress towards improved understanding of the spatial ecology of the seafloor using acoustic techniques. *Estuar Coast Shelf Sci* 92(3):502–520
- Calder BR, Mayer L (2003) Automatic processing of high-rate, high-density multibeam echosounder data. *Geochemistry, Geophysics, Geosystems* 4(6):n/a–n/a. <https://doi.org/10.1029/2002GC000486>. <http://doi.wiley.com/10.1029/2002GC000486>
- Calvert J, Strong JA, Service M, McGonigle C, Quinn R (2015) An evaluation of supervised and unsupervised classification techniques for marine benthic habitat mapping using multibeam echosounder data. *ICES Journal of Marine Science: Journal du Conseil* 72(5):1498–1513. <https://doi.org/10.1093/icesjms/fsu223>. <http://icesjms.oxfordjournals.org/content/early/2014/12/12/icesjms.fsu223.abstract>
- Chakraborty B, Kodagali V, Baracho J (2003) Sea-floor classification using multibeam echo-sounding angular backscatter data: a real-time approach employing hybrid neural network architecture. *IEEE Journal of Oceanic Engineering* 28(1):121–128. <https://doi.org/10.1109/JOE.2002.808211>
- Che Hasan R, Ierodiaconou D, Laurenson L (2012) Combining angular response classification and backscatter imagery segmentation for benthic biological habitat mapping. *Estuarine, Coastal and Shelf Science* 97(October 2015):1–9. <https://doi.org/10.1016/j.ecss.2011.10.004>. <http://linkinghub.elsevier.com/retrieve/pii/S0272771411004124>
- Che Hasan R, Ierodiaconou D, Monk J (2012) Evaluation of four supervised learning methods for benthic habitat mapping using backscatter from multi-beam sonar. *Remote Sensing* 4(11):3427–3443. <https://doi.org/10.3390/rs4113427>
- Che Hasan R, Ierodiaconou D, Laurenson L, Schimel A (2014) Integrating multibeam backscatter angular response, mosaic and bathymetry data for benthic habitat mapping. *PLoS one* 9(5):e97339. <https://doi.org/10.1371/journal.pone.0097339>
- Clarke JEH, Mayer LA, Wells DE (1996) Shallow-water imaging multibeam sonars : a new tool for investigating seafloor processes in the coastal zone and on the continental shelf. *Marine Geophysical Researches* 18(6):607–629
- Clarke JH (2003) Dynamic motion residuals : ironing out the creases. *International Hydrographic Review* (March 2003):1–30
- Copello S, Quintana F (2009) Spatio-temporal overlap between the at-sea distribution of Southern Giant Petrels and fisheries at the Patagonian Shelf. *Polar Biology* 32(8):1211–1220. <https://doi.org/10.1007/s00300-009-0620-7>
- Cutter GR, Rzhano V, Mayer LA (2003) Automated segmentation of seafloor bathymetry from multibeam echosounder data using local fourier histogram texture features. *Journal of Experimental Marine Biology and Ecology* 285–286:355–370. [https://doi.org/10.1016/S0022-0981\(02\)00537-3](https://doi.org/10.1016/S0022-0981(02)00537-3)
- Desiage PA, Montero-Serrano JC, St-Onge G, Crespi-Abril AC, Giarratano E, Gil MN, Haller M (2018) Quantifying sources and transport pathways of surface sediments in the gulf of San Jorge, Central Patagonia (Argentina). *Oceanography* 31
- Diesing M, Stephens D (2015) A multi-model ensemble approach to seabed mapping. *Journal of Sea Research* 100:62–69. <https://doi.org/10.1016/j.seares.2014.10.013>
- Eaton JW, Bateman D, Hauberg S, Wehbring R (2019) GNU octave version 5.1.0 manual: a high-level interactive language for numerical computations. <https://www.gnu.org/software/octave/doc/v5.1.0/>
- Edwards BD, Dartnell P, Chezar H (2003) Characterizing benthic substrates of Santa Monica Bay with seafloor photography and multibeam sonar imagery. *Marine Environmental Research* 56(1–2):47–66. [https://doi.org/10.1016/S0141-1136\(02\)00324-0](https://doi.org/10.1016/S0141-1136(02)00324-0). <http://www.ncbi.nlm.nih.gov/pubmed/12648949>
- Fernández M, Roux A, Fernández E, Caló J, Marcos A, Aldacur H (2003) Grain-size analysis of surficial sediments from Golfo San Jorge, Argentina. *Journal of the Marine Biological Association of the United Kingdom* 83(6):1193–1197. <https://doi.org/10.1017/S0025315403008488>
- Fezzani R, Berger L (2018) Analysis of calibrated seafloor backscatter for habitat classification methodology and case study of 158 spots in the bay of biscay and celtic sea. *Marine Geophysical Research* 39:169–181. <https://doi.org/10.1007/s11001-018-9342-y>

- Fonseca L, Brown C, Calder B, Mayer L, Rzhanov Y (2009) Angular range analysis of acoustic themes from Stanton Banks Ireland: a link between visual interpretation and multibeam echosounder angular signatures. *Applied Acoustics* 70(10):1298–1304. <https://doi.org/10.1016/j.apacoust.2008.09.008>. <http://linkinghub.elsevier.com/retrieve/pii/S0003682X08002028>
- Fontelles Temes C, Tavares de Macedo Dias G, Sperle Dias M (2019) Geohabitats characterization in areas of dredge sediment disposals on Rio de Janeiro continental shelf, adjacent to Guanabara Bay: Brazil. *Geo-Marine Letters*, pp 1–16. <https://doi.org/10.1007/s00367-019-00620-z>
- Galván D, Venerus L, Irigoyen A (2009) The reef-fish fauna of the Northern Patagonian Gulfs, Argentina, Southwestern Atlantic. *The Open Fish Science Journal* 2:90–98
- Gongora ME, Gonzalez-Zevallos D, Pettovello A, Mendia L (2012) Characterization of the main fisheries in San Jorge Gulf, Patagonia, Argentina/Caracterización de las Principales Pesquerías Del Golfo San Jorge Patagonia, Argentina. *Latin American Journal of Aquatic Research* 40(1):1–12
- Grandi MF, Dans SL, Crespo EA (2015) The recovery process of a population is not always the same: the case of *Otaria Flavescens*. *Marine Biology Research* 11(3):225–235. <https://doi.org/10.1080/17451000.2014.932912>
- Greene H, Yoklavich M, Sullivan D, Cailliet G (1995) A geophysical approach to classifying marine benthic habitats: monterey bay as a model. In: Workshop proceedings, applications of side-scan sonar and laser-line system in fisheries research. Special Publication, p 9
- Guisan A, Zimmermann NE (2000) Ecomod135_147. *Ecological Modelling* 135:147–186. [https://doi.org/10.1016/S0304-3800\(00\)00354-9](https://doi.org/10.1016/S0304-3800(00)00354-9), 1115
- Haller M, St-Onge G, Desiage PA, Sánchez-Carnero N (2020) Submarine images of the northern section of Golfo San Jorge, Patagonia, Argentina. In: Marine geology symposia – 21st argentine geological congress, submitted
- Hartigan JA, Wong MA (1979) Algorithm as 136: a k-means clustering algorithm. *Applied Statistics* 28:100–108. <https://doi.org/10.2307/2346830>
- Heap A, Harris P (2011) Geological and biological mapping and characterisation of benthic marine environments. *Cont Shelf Res* 31(2):S1–S3
- Ierodiaconou D, Monk J, Rattray A, Laurenson L, Versace VL (2011) Comparison of automated classification techniques for predicting benthic biological communities using hydroacoustics and video observations. *Continental Shelf Research* 31(2 SUPPL):28–38. <https://doi.org/10.1016/j.csr.2010.01.012>
- Irigoyen A, Eyraas C, Parma A (2011) Alien algae *Undaria pinnatifida* causes habitat loss for rocky reef fishes in North Patagonia. *Biological Invasions* 13:17–24
- Kanari M, Tibor T, Hall JK, Ketter T, Lang G, Schattner U (2020) Sediment transport mechanisms revealed by quantitative analyses of seafloor morphology: new evidence from multibeam bathymetry of the Israel exclusive economic zone. *Marine and Petroleum Geology* 114:104224. <https://doi.org/10.1016/j.marpetgeo.2020.104224>
- Kostylev V, Todd B, Fader G, Courtney R, Cameron G, Pickrill R (2001) Benthic habitat mapping on the Scotian Shelf based on multibeam bathymetry, surficial geology and sea floor photographs. *Marine Ecology Progress Series* 219:121–137. <https://doi.org/10.3354/meps219121>. <http://www.int-res.com/abstracts/meps/v219/p121-137/>
- Kostylev VE, Courtney RC, Robert G, Todd BJ (2003) Stock evaluation of giant scallop (*Placopecten magellanicus*) using high-resolution acoustics for seabed mapping. *Fisheries Research* 60(2-3):479–492. [https://doi.org/10.1016/S0165-7836\(02\)00100-5](https://doi.org/10.1016/S0165-7836(02)00100-5). <http://linkinghub.elsevier.com/retrieve/pii/S0165783602001005>
- Lastras G, Acosta J, Muñoz A, Canals M (2011) Submarine canyon formation and evolution in the Argentine Continental Margin between 44°30'S and 48°S. *Geomorphology* 128(3-4):116–136. <https://doi.org/10.1016/j.geomorph.2010.12.027>. <http://linkinghub.elsevier.com/retrieve/pii/S0169555X10005714>
- Le Bas TP, Huvenne VAI (2009) Acquisition and processing of backscatter data for habitat mapping - comparison of multibeam and sidescan systems. *Applied Acoustics* 70(10):1248–1257. <https://doi.org/10.1016/j.apacoust.2008.07.010>
- Lecours V, Dolan MF, Micallef A, Lucieer VL (2016) A review of marine geomorphometry, the quantitative study of the seafloor. *Hydrol Earth Syst Sci* 20(8):3207–3244. <https://doi.org/10.5194/hess-20-3207-2016>
- Lema H, Busteros A, Franchi M, Parisi C, Márquez M, Ardolino A (2001) Hoja Geología 4566-II y IV Camarones. Provincia del Chubut. Instituto de Geología y Recursos Minerales, Servicio Geológico Minero Argentino. Boletín 261, Buenos Aires
- Li D, Tang C, Xia C, Zhang H (2017) Acoustic mapping and classification of benthic habitat using unsupervised learning in artificial reef water. *Estuarine, Coastal and Shelf Science* 185:11–21. <https://doi.org/10.1016/j.ecss.2016.12.001>
- López-Martínez J, Muñoz A, Dowdeswell J, Linés C, Acosta J (2011) Relict sea-floor ploughmarks record deep-keeled Antarctic icebergs to 45°S on the Argentine margin. *Marine Geology* 288(1-4):43–48. <https://doi.org/10.1016/j.margeo.2011.08.002>. <http://linkinghub.elsevier.com/retrieve/pii/S0025322711001836>
- Lucatelli D, Goes ER, Brown CJ, Souza-Filho JF, Guedes-Silva E, Araujo TCM (2019) Geodiversity as an indicator to benthic habitat distribution: an integrative approach in a tropical continental shelf. *Geo-Marine Letters*. <https://doi.org/10.1007/s00367-019-00614-x>
- Lurton X, Eleftherakis D, Augustin JM (2018) Analysis of seafloor backscatter strength dependence on the survey azimuth using multibeam echosounder data. *Mar Geophys Res* 39:183–203. <https://doi.org/10.1007/s11001-017-9318-3>
- Madirolas A, Isla F, Tripode M, Colombo GA, Cabreira A (2005) First results from the multibeam surveys carried out over the argentine continental shelf. In: FEMME, Dublin, Ireland, pp 26–29
- Mcgonigle C, Brown C, Quinn R, Grabowski J (2009) Evaluation of image-based multibeam sonar backscatter classification for benthic habitat discrimination and mapping at Stanton Banks, UK. *Estuarine, Coastal and Shelf Science* 81(3):423–437. <https://doi.org/10.1016/j.ecss.2008.11.017>
- Micallef A, Le Bas TP, al Huvenne V, Blondel P, Hühnerbach V, Deidun A (2012) A multi-method approach for benthic habitat mapping of shallow coastal areas with high-resolution multibeam data. *Continental Shelf Research* 39-40:14–26. <https://doi.org/10.1016/j.csr.2012.03.008>. <http://linkinghub.elsevier.com/retrieve/pii/S0278434312000726>
- Misiuk B, Lecours V, Bell T (2018) A multiscale approach to mapping seabed sediments. *PLOS ONE* 13(2):e0193647. <https://doi.org/10.1371/journal.pone.0193647>
- Nievas M, Esteves J (2007) Relevamiento de actividades relacionadas con la explotación de petróleo en la zona costera patagónica y datos preliminares sobre residuos de hidrocarburos en puertos proyecto arg/02/g31-pnud-gef. Tech. rep., Patagonia Natural Foundation
- Normandeau A, Lajeunesse P, St-Onge G, Bourgault D, St-Onge Drouin S, Senneville S, Bélanger S (2014) Morphodynamics in sediment-starved inner-shelf submarine canyons (Lower St. Lawrence Estuary, Eastern Canada). *Marine Geology* 27:243–255. <https://doi.org/10.1016/j.margeo.2014.08.012>
- Normandeau A, Lajeunesse P, St-Onge G (2015) Submarine canyons and channels in the lower st. lawrence estuary (eastern canada): morphology, classification and recent sediment dynamics.

- Geomorphology 241:1–18. <https://doi.org/10.1016/j.geomorph.2015.03.023>
- Pandian P, Ruscoe J, Shields M, Side J, Harris R, Kerr S, Bullen C (2009) Seabed habitat mapping techniques: an overview of the performance of various systems. *Mediterranean Marine Science* 10(2):29–44
- Pankhurst R, Leat P, P S Rapela C, Márquez M, Storey B, Riley T (1998) The chon aike province of patagonia and related rocks in westantarctica: a silicic large igneous province. *J Volcanol Geotherm Res* 81:113–136
- Parnum I, Siwabessy P, Gavrilov A (2004) Identification of seafloor habitats in coastal shelf waters using a Multibeam echosounder. In: *ACOUSTICS 2004, Gold coast, Australia, November*, pp 181–186
- Picard K, Brooke BP, Harris PT, Siwabessy PJW, Tran M, Spinocchia M, Weales J, Macmillan-lawler M, Sullivan J (2018) Malaysia Airlines flight MH370 search data reveal geomorphology and seafloor processes in the remote southeast Indian Ocean. *Marine Geology* 395(July 2017):301–319. <https://doi.org/10.1016/j.margeo.2017.10.014>
- Pickrill R, Todd BJ (2003) The multiple roles of acoustic mapping in integrated ocean management, Canadian Atlantic continental margin. *Ocean & Coastal Management* 46(6-7):601–614. [https://doi.org/10.1016/S0964-5691\(03\)00037-1](https://doi.org/10.1016/S0964-5691(03)00037-1)
- Pillay T, Cawthra HC, Lombard AT (2020) Characterisation of seafloor substrate using advanced processing of multibeam bathymetry, backscatter, and sidescan sonar in Table Bay, South Africa. *Marine Geology*. [10.1016/j.margeo.2020.106332](https://doi.org/10.1016/j.margeo.2020.106332)
- Pirtle JL, Weber TC, Wilson CD, Rooper CN (2015) Assessment of trawlable and untrawlable seafloor using multibeam-derived metrics. *Methods in Oceanography* 12:18–35. <https://doi.org/10.1016/j.mio.2015.06.001>
- R Core Team (2019) R: a language and environment for statistical computing. R Foundation for Statistical Computing, Vienna, Austria. <https://www.R-project.org/>
- Rattray A, Ierodiaconou D, Laurenson L, Burq S, Reston M (2009) Hydro-acoustic remote sensing of benthic biological communities on the shallow South East Australian continental shelf. *Estuarine, Coastal and Shelf Science* 84(2):237–245. <https://doi.org/10.1016/j.ecss.2009.06.023>
- Rattray A, Ierodiaconou D, Monk J, Versace V, Laurenson L (2013) Detecting patterns of change in benthic habitats by acoustic remote sensing. *Marine Ecology Progress Series* 477:1–13. <https://doi.org/10.3354/meps10264>. <http://www.int-res.com/abstracts/meps/v477/p1-13/>
- Roberts J, Brown C, Long D, Bates C (2005) Acoustic mapping using a multibeam echosounder reveals cold-water coral reefs and surrounding habitats. *Coral Reefs* 24(4):654–669. <https://doi.org/10.1007/s00338-005-0049-6>. <http://link.springer.com/10.1007/s00338-005-0049-6>
- Romero MA, Grandi MF, Koen-Alonso M, Svendsen G, Ocampo Reinaldo M, García NA, Dans SL, González R, Crespo EA (2017) Analysing the natural population growth of a large marine mammal after a depletive harvest. *Scientific Reports* 7(1):1–16. <https://doi.org/10.1038/s41598-017-05577-6>
- Shumchenia E, King J (2010) Comparison of methods for integrating biological and physical data for marine habitat mapping and classification. *Cont Shelf Res* 30(16):1717–1729
- Simons DG, Snellen M (2009) A Bayesian approach to seafloor classification using multi-beam echo-sounder backscatter data. *Applied Acoustics* 70(10):1258–1268. <https://doi.org/10.1016/j.apacoust.2008.07.013>. <http://linkinghub.elsevier.com/retrieve/pii/S0003682X08001813>
- Singh H, Adams J, Mindell D, Foley B (2006) Imaging underwater for archaeology. *Journal of Field Archaeology* 27(3):319. <https://doi.org/10.2307/530446>
- St-Onge G, Ferreyra GA (2018) Introduction to the special issue on the gulf of San Jorge (Patagonia, Argentina). *Oceanography* 31:14–15. <https://doi.org/10.5670/oceanog.2018.406>
- Stephens D, Diesing M (2014) A comparison of supervised classification methods for the prediction of substrate type using multibeam acoustic and legacy grain-size data. *PLoS ONE* 9(4). <https://doi.org/10.1371/journal.pone.0093950>
- Trobiani G (2018) La pesca de arrastre en la costa norte del golfo san jorge: distribución frecuencia de disturbio y efectos sobre las comunidades asociadas al fondo. PhD thesis, Universidad de Comahue
- Trobiani G, Irigoyen A (2016) pepe: a novel low cost drifting video system for underwater survey. In: 3rd IEEE/OES South American international symposium on oceanic engineering (SAISOE), pp 1–4
- Van De Beuque S, Auzende JM, Lafoy Y, Grandperrin R (1999) Benefits of swath mapping for the identification of marine habitats in the New Caledonia Economic Zone. *Oceanologica Acta* 22(6):641–650
- Whitmire CE, Embley RW, Wakefield WW, Merle SG, Tissot BN (2007) A quantitative approach for using multibeam sonar data to map benthic habitats. *Mapping the Seafloor for Habitat Characterization: Geological Association of Canada, Special Paper* 47:111–126
- Wilson MFJ, O’Connell B, Brown C, Guinan JC, Grehan AJ (2007) Multiscale terrain analysis of multibeam bathymetry data for habitat mapping on the continental slope. *Marine Geodesy* 30(1-2):3–35. <https://doi.org/10.1080/01490410701295962>. <http://www.tandfonline.com/doi/abs/10.1080/01490410701295962>
- Yang F, Li J, Wu Z, Jin X, Chu F, Kang Z (2007) A post-processing method for the removal of refraction artifacts in multibeam bathymetry data. *Marine Geodesy - MAR GEODESY* 30:235–247. <https://doi.org/10.1080/01490410701438380>
- Yorio P (2000) Breeding seabirds of argentina: conservation tools for a more integrated and regional approach. *Emu* 100(5 SUPPL):367–375. <https://doi.org/10.1071/MU0004S>
- Yorio P (2009) Marine protected areas, spatial scales, and governance: implications for the conservation of breeding seabirds. *Conserv Lett* 2(4):171–178. <https://doi.org/10.1111/j.1755-263x.2009.00062.x>

Publisher’s note Springer Nature remains neutral with regard to jurisdictional claims in published maps and institutional affiliations.